

# MirrorLimb: Implementing hand pose acquisition and robot teleoperation based on RealMirror

Cong Tai† Hansheng Wu† Haixu Long Zhengbin Long  
Zhaoyu Zheng Haodong Xiang Tao Shen\*  
ZTE Terminators Group

 <https://github.com/terminators2025/RealMirror>

## Abstract

In this work, we present a PICO-based robot remote operating framework that enables low-cost, real-time acquisition of hand motion and pose data, outperforming mainstream visual tracking and motion capture solutions in terms of cost-effectiveness. The framework is natively compatible with the RealMirror ecosystem, offering ready-to-use functionality for stable and precise robotic trajectory recording within the Isaac simulation environment, thereby facilitating the construction of Vision-Language-Action (VLA) datasets. Additionally, the system supports real-time teleoperation of a variety of end-effector-equipped robots, including dexterous hands and robotic grippers. This work aims to lower the technical barriers in the study of upper-limb robotic manipulation, thereby accelerating advancements in VLA-related research.

## 1 Introduction

Recently, Vision-Language-Action (VLA) models have become a research hotspot in the field of robotics. Many of these models demonstrate impressive upper-limb manipulation capabilities in robots (Zhao et al., 2023; Chi et al., 2023; Figure AI, 2025; Black et al., 2024; Shukor et al., 2025). To enable more systematic evaluation and evolution of VLA models, related work—RealMirror provides an end-to-end VLA research platform integrating data collection, training, and evaluation (Tai et al., 2025). Within RealMirror, teleoperation data from multiple simulation scenarios serves as the cornerstone of the workflow. Experimental results indicate that the quality and diversity of human demonstrations directly determine the performance of VLA models (Yang et al., 2025).

Currently, several mainstream paradigms exist for mapping human motions to robot embodiments. One approach involves using professional motion capture systems: motion data captured from sensors is processed in real time and directly mapped to the corresponding joints of the robot. This method can capture joint angle ground truths with high fidelity, but high hardware costs and issues such as joint drift limit its widespread adoption. Another approach relies on the interactive capabilities of XR or visual devices (Cheng et al., 2024; Qin et al., 2023), mapping motion data from handle or human hands. For XR teleoperation schemes using handles, while the end-pose of the handle can be acquired stably, the grasping actions of the robot are often limited to predefined functional packages, resulting in relatively monotonous movements and a lack of fine manipulation capabilities. For vision-based XR mapping schemes, such as the Apple Vision Pro teleoperation system integrated into the IsaacLab ecosystem (Lab, 2025), although expensive wearable hardware is avoided, the Apple Vision Pro remains costly. Moreover, acquiring stable and accurate real-time hand joint poses remains a significant challenge. To address these challenges, we have extended the capabilities of RealMirror’s handle-based teleoperation by proposing MirrorLimb—a control system

† Equal contribution

\* Corresponding author. Emails: shen.tao5@zte.com.cn

based on PICO devices for robot teleoperation via hand gestures or handles. The main contributions of this system are as follows:

- 1) Native compatibility with the RealMirror platform. Combined with RealMirror’s kinematic/dynamic optimization capabilities for robot motion resolution, it enables highly precise and stable remote robot teleoperation within the IsaacSim simulation environment.
- 2) Integration of a WebXR/OpenXR-based communication framework and an end-to-end teleoperation software system—providing standardized interfaces for mapped raw data from handle/gesture inputs, facilitating adaptation to different operating platforms and various robot end-effectors.
- 3) MirrorLimb supports XR devices such as PICO 3 & 4, offering significantly more cost-effective hardware compared to motion capture systems or Apple Vision Pro, thereby substantially lowering the barrier to achieving fine-grained robotic manipulation.

## 2 Data Acquisition And Kinematic Optimization

We design a dual-channel acquisition stack that captures both handle commands and fine-grained hand gestures from PICO XR devices in real time. The handle path is implemented with WebXR in a browser runtime and streamed to a secure Node.js server, while the gesture path uses OpenXR (via PICO’s Unity SDK) and transmits fixed-rate joint poses via UDP. Both streams are normalized to the RealMirror/IsaacSim coordinate conventions and exposed through standardized schemas for downstream VLA data curation and teleoperation. The handle and gesture teleoperation diagram is shown in Figure 1.



Figure 1: Handle and gesture teleoperation demonstration.

### 2.1 Architectural Overview

- The acquisition pipeline prioritizes low latency, stability, and cost-efficiency.
- WebXR handle data are sampled in the XR frame loop without rendering overhead, quantized, and pushed over a persistent socket to a server that performs atomic file updates for consumers in IsaacSim/RealMirror.
- OpenXR hand joint poses are sampled at a fixed 60 Hz independent of rendering, serialized into a compact binary payload, and sent via UDP to minimize end-to-end latency.

### 2.2 WebXR-Based Handle Acquisition

The handle acquisition path is implemented within a browser runtime using WebXR, prioritizing efficiency and robustness. To minimize system overhead, an XR session is initiated without performing any scene rendering; its frame loop is used exclusively to drive data capture at the device’s native refresh rate (typically 72–90 Hz). For each frame, the system queries the 6-DoF poses for both

the grip space (handle body) and the target ray space (pointer), alongside the state of all buttons and joystick axes.

A critical step in this process is coordinate system harmonization. Poses originating from the WebXR runtime (a right-handed, Y-up frame) are transformed into IsaacSim’s right-handed, Z-up world convention. This involves a consistent change of basis for both position and orientation to ensure seamless integration. To enhance control stability and reduce network bandwidth, position data is quantized to 1 mm resolution. The resulting data stream is then transmitted over a secure and persistent WebSocket (Socket.IO) connection. On the server, data integrity is guaranteed through an atomic write mechanism, where the latest frame is written to a temporary file before being renamed, thus preventing downstream consumers in RealMirror from accessing incomplete data.

### 2.3 OpenXR/Unity-Based Hand Gesture Acquisition

To capture fine-grained hand motions, we leverage PICO’s native OpenXR APIs within the Unity engine. This path provides per-frame 3D position and orientation for all 26 tracked joints of each hand, enabling the system to represent dexterous manipulation. The mapping of these joints and their native left-handed coordinate system is illustrated in Figure 2. A key architectural choice is the decoupling of data sampling from the rendering loop. We enforce a fixed 60 Hz transmission rate, which ensures temporally consistent data intervals. This stability is crucial for both reliable real-time teleoperation and the construction of reproducible, high-quality datasets.

The coordinate transformation for the gesture stream is more complex than that of the handle stream. As noted, poses from the PICO Unity/OpenXR path are reported in a left-handed coordinate system. Therefore, they first undergo a handedness normalization to a right-handed system before being remapped to IsaacSim’s Z-up convention. For network transport, each hand’s joint data is serialized into a compact binary payload and transmitted via UDP. The choice of UDP as the transport protocol is motivated by the stream’s high-frequency nature, which allows for tolerance to occasional packet loss. This trade-off is well-suited for real-time control applications.

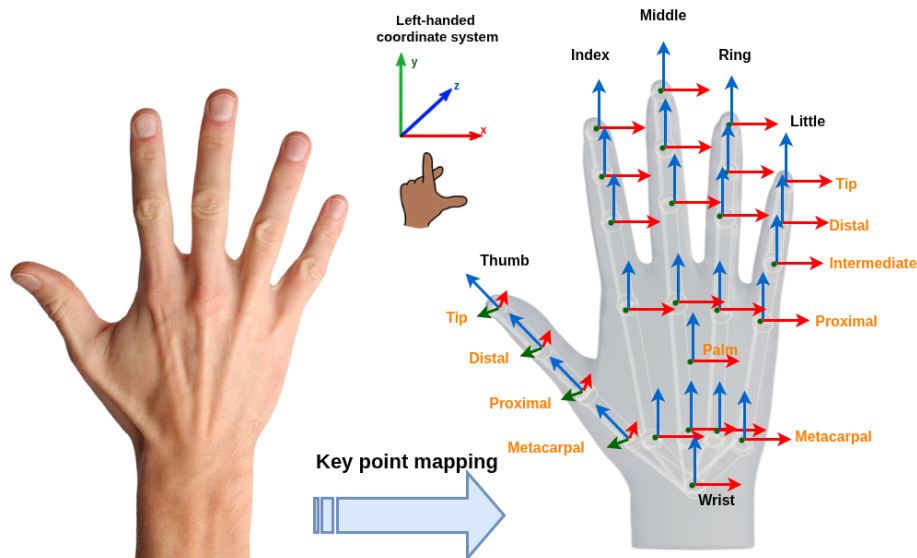


Figure 2: The mapping and coordinate system representation of hand tracking.

## 2.4 Reliability, Security, and Resource Efficiency

- Reliability: The WebXR path re-establishes reference spaces on loss and handles session termination cleanly. The server persists only the latest frame and performs atomic writes to eliminate partial-file reads.
- Security: WebXR runs in a secure context (HTTPS), and the transport uses authenticated TLS, satisfying browser policy and reducing attack surface in LAN deployment.
- Efficiency: Minimal rendering eliminates GPU load during acquisition; quantization reduces bandwidth and numerical jitter; UDP binary streaming for hands minimizes serialization overhead.

## 2.5 Data Post-processing

In the field of robot teleoperation, end-effector jitter and sudden jumps are common issues. Specifically, one cause of jitter stems from biological tremor, meaning the human hand cannot remain completely stationary in space, resulting in inherent jitter in the raw data (Dai et al., 2020). Another cause of jitter is related to the nature of the Inverse Kinematics (IK) solver. When the positional displacement between two consecutive calculations is too small, the IK solution may still produce noticeable jitter in the end-effector (Buss, 2004).

Regarding sudden jumps, there are also two primary causes. Firstly, unstable raw data transmission or fluctuations in hand pose estimation can lead to significant jumps in the data. Secondly, the IK solver may encounter singularities or multiple solution scenarios, causing large, abrupt jumps in the end-effector's position (Guenther et al., 2008).

To effectively mitigate control instability induced by jitter and jumps, we designed a series of rules for kinematic optimization during the IK solving stage. This is achieved by filtering potential end-effector jitter and jumps between consecutive frames.

These related parameters are defined as:  $t$  represents the current frame time index;  $\mathbf{p}_t$  represents the position vector of the original end-effector of the current frame (from PICO parsing);  $\theta_t = [\theta_{t,1}, \theta_{t,2}, \dots, \theta_{t,m}]$  represents the original joint angle vector of the current frame (joint1 to jointm);  $\phi_t = [\phi_{t,1}, \phi_{t,2}, \dots, \phi_{t,m}]$  represents the joint angle control signal vector after IK calculation in the current frame; The end position change vector is represented by the Euclidean distance between adjacent frames of the end joint:  $\Delta \mathbf{p}_t = \mathbf{p}_t - \mathbf{p}_{t-1}$ ,  $d_t = \|\Delta \mathbf{p}_t\|$ ;  $\Delta \theta_{t,i} = |\theta_{t,i} - \theta_{t-1,i}|$  represents the absolute value of the inter frame change in the  $i$  original joint angle ( $i = 1, \dots, m$ );  $\Delta \phi_{t,i} = |\phi_{t,i} - \phi_{t-1,i}|$  represents the absolute value of the inter frame variation of the  $i$  IK solved joint angle ( $i = 1, \dots, m$ );  $\delta_1$  represents the first layer jitter filtering threshold (end distance);  $\delta_2$  represents the second layer jitter filtering threshold (end distance, used for IK solvers);  $\epsilon_1$  represents the third-layer jump filtering threshold (original joint angle);  $\epsilon_2$  represents the fourth layer jump filtering threshold (IK calculated joint angle).

The filtering rules are defined as follows:

$$d_t \geq \delta_1 \text{ (First-layer Jitter Filter)} \quad (1)$$

$$d_t \geq \delta_2 \text{ (Second-layer Jitter Filter)} \quad (2)$$

$$\max_{i=1}^m \Delta \theta_{t,i} \leq \epsilon_1 \text{ (Third-layer Jump Filter (Raw Data))} \quad (3)$$

$$\max_{i=1}^m \Delta \phi_{t,i} \leq \epsilon_2 \text{ (Fourth-layer Jump Filter (IK Solution))} \quad (4)$$

Executable data flag  $E_t$  indicates whether the current frame data is executable:

$$E_t = \begin{cases} 1 & \text{when } (d_t \geq \delta_1) \wedge (d_t \geq \delta_2) \wedge (\max_{i=1}^m \Delta \theta_{t,i} \leq \epsilon_1) \wedge (\max_{i=1}^m \Delta \phi_{t,i} \leq \epsilon_2), \\ 0 & \text{otherwise,} \end{cases} \quad (5)$$

Through the aforementioned kinematic optimization, jitter and sudden jumps of the end-effector during teleoperation can be effectively suppressed. This optimization is natively integrated into the RealMirror platform, enabling optimal control performance whether using a handle or gesture-based input.

### 3 Integration with RealMirror VLA Ecosystem

To ensure broad applicability and optimal performance of MirrorLimb, we have natively integrated its gesture and handle-based teleoperation capabilities into RealMirror. Furthermore, we have standardized and exposed the MirrorLimb data interfaces. The complete end-to-end teleoperation workflow is illustrated in Figure 3.

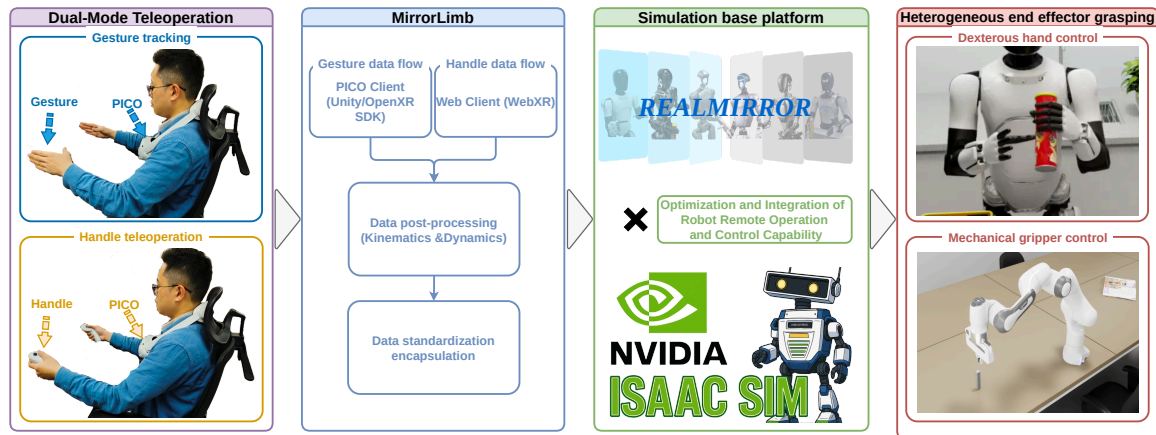


Figure 3: Robot teleoperation system framework based on RealMirror ecosystem.

The workflow incorporates two selectable teleoperation modes. Empirical findings indicate that handle-based operation yields optimal data acquisition efficiency for simple tasks involving repetitive motions, whereas gesture proves more advantageous for complex tasks demanding continuous hand pose adjustments during data collection. The MirrorLimb system processes acquired gesture or handle data streams through subsequent data post-processing and kinematic optimization before integration into the RealMirror platform. On the robot side, kinematic constraints and dynamic optimizations have also been implemented to enhance compatibility with the MirrorLimb data stream, thereby achieving more stable robot control.

#### 3.1 Structured Gesture Data Flow

To interface the teleoperation data flow with RealMirror, we have designed a standardized data interface. The structure of the gesture data stream is summarized in Table 1.

It is worth noting that each recognizable joint is represented by position coordinates and a quaternion to convey its pose and orientation. The "handedness" label indicates whether the data corresponds to the left or right hand. The pose of the "Wrist" joint is selected as the representative pose for the entire hand.

#### 3.2 Structured Handle Data Flow

In contrast to the gesture data flow, while maintaining the same basic structure and key names, the handle data flow contains several unique parameters. The "profiles" field specifies a list of supported handle profiles or hardware identifiers, such as "oculus-touch-v2", "pico-phoenix", "pico-neo3", "pico-neo2", "oculus-touch", and "generic-trigger-squeeze-thumbstick". Furthermore, the

Field Name	Data Type	Description
<b>(Root)</b>	<b>Object</b>	<b>The root object representing a single data frame.</b>
timestamp	Integer	Unix timestamp of the data frame.
data	Array<Object>	An array containing one or more 'Hand' objects.
<b>Hand Object</b>	<b>Object</b>	<b>Describes the complete information of a single hand.</b>
id	String	Unique identifier for the hand in the current frame.
handedness	String	Handedness ('left' or 'right').
pose	Object	The overall pose object of the hand.
position	Array<Float>	3D position '[x, y, z]'.
orientation	Array<Float>	Orientation as a quaternion '[x, y, z, w]'.
joints	Array<Object>	An array of 26 'Joint' objects.
<b>Joint Object</b>	<b>Object</b>	<b>Describes a single hand joint.</b>
name	String	Name of the joint (e.g., 'Palm', 'ThumbTip').
position	Array<Float>	The joint's 3D position '[x, y, z]'.
orientation	Array<Float>	The joint's orientation as a quaternion '[x, y, z, w]'.

Table 1: Gesture tracking structured data.

extensive button information on the handle must be transmitted via the data stream to ensure precise handle-based teleoperation. This is particularly crucial for fine-tuning the robot wrist's roll, yaw, and pitch during teleoperation, which is achieved through specific handle buttons. The complete structure of the handle data flow is detailed in Table 2.

Field Name	Data Type	Description
<b>(Root)</b>	<b>Object</b>	<b>The root object for a single input data frame.</b>
timestamp	Integer	Unix timestamp of the data frame.
data	Array<Object>	An array containing one or more handle objects.
<b>handle Object</b>	<b>Object</b>	<b>Describes a single input handle.</b>
id	String	Unique identifier for the handle (e.g., 'right').
handedness	String	Specifies the handedness ('left' or 'right').
profiles	Array<String>	A list of supported handle profiles or hardware identifiers.
buttons	Array<Object>	An array of Button State objects, indexed by button type.
axes	Array<Float>	An array representing the state of analog axes (e.g., thumbsticks).
pose	Object	The physical pose of the handle in 3D space.
position	Array<Float>	3D position as '[x, y, z]'.
orientation	Array<Float>	Orientation as a quaternion '[x, y, z, w]'.
targetRayPose	Object	The pose of the handle's targeting ray for pointing.
position	Array<Float>	3D position of the ray's origin.
orientation	Array<Float>	Direction of the ray represented as a quaternion.
<b>Button State Object</b>	<b>Object</b>	<b>Describes the state of a single button.</b>
pressed	Boolean	True if the button is currently being fully pressed.
touched	Boolean	True if the button is being touched (for capacitive sensors).
value	Float	The analog value of the button/trigger, typically from 0.0 to 1.0.

Table 2: Handle tracking structured data.

## 4 Conclusion

In this work, we have presented MirrorLimb, a cost-effective and robust framework for real-time hand pose acquisition and robot teleoperation, built upon the RealMirror ecosystem. By leveraging PICO XR devices, MirrorLimb effectively addresses the limitations of existing motion capture and visual tracking solutions, offering high-precision data acquisition through dual-channel streams based on WebXR and OpenXR protocols. The system natively integrates with IsaacSim, enabling stable trajectory recording and dexterous manipulation for VLA dataset construction. Through kinematic optimization, we effectively mitigate end-effector jitter and sudden jumps, ensuring reliable teleoperation performance. The standardized data interfaces for both gesture and handle inputs facilitate seamless adaptation to diverse robotic end-effectors, lowering the barrier for upper-limb manipulation research.

MirrorLimb’s compatibility with RealMirror not only accelerates VLA-related advancements but also provides a scalable platform for future explorations in embodied AI. Moving forward, we aim to extend support to additional XR devices and enhance real-time adaptability for complex manipulation tasks.

## References

- Kevin Black, Noah Brown, Danny Driess, Adnan Esmail, Michael Equi, Chelsea Finn, Niccolo Fusai, Lachy Groom, Karol Hausman, Brian Ichter, et al. *pi.0: A vision-language-action flow model for general robot control*. *arXiv preprint arXiv:2410.24164*, 2024.
- Samuel R Buss. Introduction to inverse kinematics with jacobian transpose, pseudoinverse and damped least squares methods. *IEEE Journal of Robotics and Automation*, 17(1-19):16, 2004.
- Xuxin Cheng, Jialong Li, Shiqi Yang, Ge Yang, and Xiaolong Wang. Open-television: Teleoperation with immersive active visual feedback. *arXiv preprint arXiv:2407.01512*, 2024.
- Cheng Chi, Zhenjia Xu, Siyuan Feng, Eric Cousineau, Yilun Du, Benjamin Burchfiel, Russ Tedrake, and Shuran Song. Diffusion policy: Visuomotor policy learning via action diffusion. *The International Journal of Robotics Research*, pp. 02783649241273668, 2023.
- Jiandong Dai, Zhijiang Du, Zhiyuan Yan, and Yunlei Liang. Least squares support vector machine kalman filter for physiological tremor suppression in minimally invasive surgical robot. *Journal of Harbin Institute of Technology (New Series)*, 27(5):22–28, 2020.
- Figure AI. Helix: A vision-language-action model for generalist humanoid control, February 2025. URL <https://www.figure.ai/news/helix>.
- Raul Guenther, H Simas, D da Cruz, and D Martins. A new integration method for differential inverse kinematics of closed-chain robots. In *ACBM Symposium Series In Mechatronics*, volume 3, pp. 225–235, 2008.
- Isaac Lab. Cloudxr teleoperation, 2025. URL [https://isaac-sim.github.io/IsaacLab/main/source/how-to/cloudxr\\_teleoperation.html#cloudxr-teleoperation](https://isaac-sim.github.io/IsaacLab/main/source/how-to/cloudxr_teleoperation.html#cloudxr-teleoperation).
- Yuzhe Qin, Wei Yang, Binghao Huang, Karl Van Wyk, Hao Su, Xiaolong Wang, Yu-Wei Chao, and Dieter Fox. Anyteleop: A general vision-based dexterous robot arm-hand teleoperation system. *arXiv preprint arXiv:2307.04577*, 2023.
- Mustafa Shukor, Dana Aubakirova, Francesco Capuano, Pepijn Kooijmans, Steven Palma, Adil Zouitine, Michel Aractingi, Caroline Pascal, Martino Russi, Andres Marafioti, et al. Smolvla: A vision-language-action model for affordable and efficient robotics. *arXiv preprint arXiv:2506.01844*, 2025.

Cong Tai, Zhaoyu Zheng, Haixu Long, Hansheng Wu, Haodong Xiang, Zhengbin Long, Jun Xiong, Rong Shi, Shizhuang Zhang, Gang Qiu, et al. Realmirror: A comprehensive, open-source vision-language-action platform for embodied ai. *arXiv preprint arXiv:2509.14687*, 2025.

Rushuai Yang, Hangxing Wei, Ran Zhang, Zhiyuan Feng, Xiaoyu Chen, Tong Li, Chuheng Zhang, Li Zhao, Jiang Bian, Xiu Su, et al. Beyond human demonstrations: Diffusion-based reinforcement learning to generate data for vla training. *arXiv preprint arXiv:2509.19752*, 2025.

Tony Z Zhao, Vikash Kumar, Sergey Levine, and Chelsea Finn. Learning fine-grained bimanual manipulation with low-cost hardware. *arXiv preprint arXiv:2304.13705*, 2023.